

AFAPL-TR-75-97

27

AD A 038599

# MHD POWER GENERATION (VIKING SERIES) WITH HYDROCARBON FUELS

AVCO EVERETT RESEARCH LABORATORY, INC  
2385 REVERE BEACH PARKWAY  
EVERETT, MASSACHUSETTS 02149

SEPTEMBER 1975

TECHNICAL REPORT AFAPL-TR-75-97  
FINAL REPORT FOR PERIOD 7 APRIL 1975 - 15 AUGUST 1975

DDC  
RECEIVED  
APR 26 1976  
RECEIVED

QV

C

Approved for public release; distribution unlimited

AD No. \_\_\_\_\_  
DDC FILE COPY

AIR FORCE AERO PROPULSION LABORATORY  
AIR FORCE WRIGHT AERONAUTICAL LABORATORIES  
AIR FORCE SYSTEMS COMMAND  
WRIGHT-PATTERSON AIR FORCE BASE, OHIO 45433

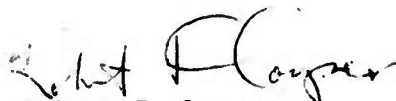
NOTICE

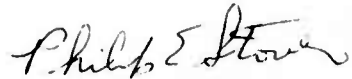
When Government drawings, specifications, or other data are used for any purpose other than in connection with a definitely related Government procurement operation, the United States Government thereby incurs no responsibility nor any obligation whatsoever; and the fact that the government may have formulated, furnished, or in any way supplied the said drawings, specifications, or other data, is not to be regarded by implication or otherwise as in any manner licensing the holder or any other person or corporation, or conveying any rights or permission to manufacture, use, or sell any patented invention that may in any way be related thereto.

This final report was submitted by Avco Everett Research Laboratory, Inc., under Contract F33615-75-C-2047. The effort was sponsored by the Air Force Aero Propulsion Laboratory, Air Force Systems Command, Wright-Patterson AFB, Ohio under Advanced Research Projects Agency, Project No. 2357 and Aero Propulsion Laboratory Project No. 3145, Task No. 26 and Work Unit No. 24 with Project Engineer Robert F. Cooper/AFAPL/POP-2 as Project Engineer In-Charge. Contract Project Scientist Robert Kessler of Avco Everett Research Laboratory, Inc., was technically responsible for the work.

This report has been reviewed by the Information Office, (ASD/OIP) and is releasable to the National Technical Information Service (NTIS). At NTIS, it will be available to the general public, including foreign nations.

This technical report has been reviewed and is approved for publication.

  
Robert F. Cooper  
High Power Program Manager

  
Philip E. Stover  
High Power Branch Chief

FOR THE COMMANDER

Copies of this report should not be returned unless return is required by security considerations, contractual obligations, or notice on a specific document.

AIR FORCE

ADMISSION	NTIS	White Service	Ball Service
DATE	PROJECT	PROJECT	PROJECT
DATE	PROJECT	PROJECT	PROJECT
DATE	PROJECT	PROJECT	PROJECT

A

UNCLASSIFIED

SECURITY CLASSIFICATION OF THIS PAGE (When Data Entered)

REPORT DOCUMENTATION PAGE		READ INSTRUCTIONS BEFORE COMPLETING FORM
1. REPORT NUMBER AFAPL-TR-75-97	2. GOVT ACCESSION NO.	3. RECIPIENT'S CATALOG NUMBER
4. TITLE (and Subtitle) MHD POWER GENERATION (VIKING SERIES) WITH HYDROCARBON FUELS	5. TYPE OF REPORT & PERIOD COVERED Final Technical Report. April 7, 75 - August 15, 75	6. PERFORMING ORG. REPORT NUMBER 7 Apr - 15 Aug 75
7. AUTHOR(s) Robert A. Kessler	8. CONTRACT OR GRANT NUMBER(s) F33615-75-C-2047, new ARPA Order - 2357	9. PROGRAM ELEMENT, PROJECT, TASK AREA & WORK UNIT NUMBERS Project No. 3145 Task No. 26 Work Unit No. 24
10. PERFORMING ORGANIZATION NAME AND ADDRESS Avco Everett Research Laboratory, Inc. 2385 Revere Beach Parkway Everett, Massachusetts 02149	11. CONTROLLING OFFICE NAME AND ADDRESS Advanced Research Projects Agency ARPA Order No. 2357	12. REPORT DATE September 1975
13. MONITORING AGENCY NAME & ADDRESS (if different from Controlling Office) Air Force Aero-Propulsion Laboratory Air Force Wright Aeronautical Laboratories Air Force Systems Command Wright-Patterson Air Force Base, Ohio 45433	14. SECURITY CLASS. (of this report) Unclassified	15. NUMBER OF PAGES 33
16. DISTRIBUTION STATEMENT (of this Report) Approved for public release; distribution unlimited.		15a. DECLASSIFICATION/DOWNGRADING SCHEDULE
17. DISTRIBUTION STATEMENT (of the abstract entered in Block 20, if different from Report) 3145 / 26		
18. SUPPLEMENTARY NOTES		
19. KEY WORDS (Continue on reverse side if necessary and identify by block number) 1. High Performance MHD Burners 2. High Performance MHD Generator 3. Compact MHD Generator 4. Burst Power Supply 5. Fast Start Power Systems 6. Direct Energy Conversion Systems 7. MHD Generators		
20. ABSTRACT (Continue on reverse side if necessary and identify by block number) The design, fabrication and operation of a compact high-performance burner for a two megawatt MHD generator is described. The burner was designed to operate on hydrocarbon fuels and oxygen, with cesium seed, at mass flow rates up to 2.7 kg/sec, chamber pressures up to 15 atmospheres and with rapid start capability. The burner was operated to about 90% of its design mass flow and chamber pressure. Operation at higher flow rates was restricted by limitations of the test facility. Measured heat losses at high flow rates were approximately 9% of the enthalpy input. Starting times, to full chamber pressure, were		

DD FORM 1 JAN 73 1473

EDITION OF 1 NOV 65 IS OBSOLETE

UNCLASSIFIED

SECURITY CLASSIFICATION OF THIS PAGE (When Data Entered)

048450

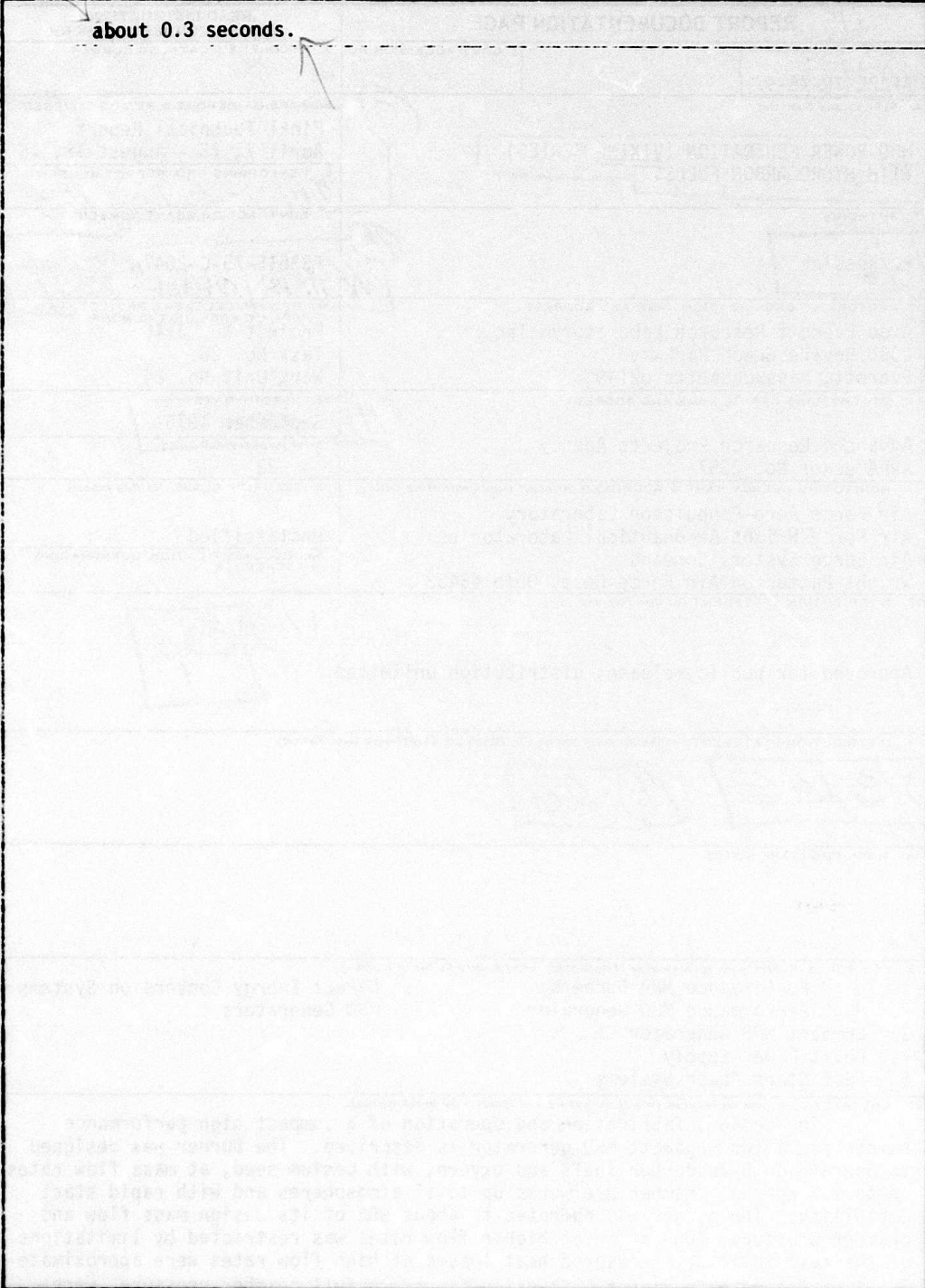
JB

*Contd*

**UNCLASSIFIED**

SECURITY CLASSIFICATION OF THIS PAGE(When Data Entered)

about 0.3 seconds.



UNCLASSIFIED  
SECURITY CLASSIFICATION OF THIS PAGE(When Data Entered)

## TABLE OF CONTENTS

<u>Section</u>		<u>Page</u>
	List of Illustrations	ii
I	INTRODUCTION, SUMMARY AND CONCLUSIONS	1
II	BURNER DESIGN, FABRICATION AND INSTALLATION	3
	A. Introduction	3
	B. Overall Design Considerations	3
	C. Detailed Design	7
III	TEST PROGRAM	19
	A. Test Facility	19
	B. Burner Tests	23
	C. Conductivity Measurements	31
	REFERENCES	33

## LIST OF ILLUSTRATIONS

<u>Figure</u>		<u>Page</u>
1	Conductivity as a Function of Overall Burner Loss	4
2	VIKING I Combustion Chamber Length	6
3	VIKING I Compact Burner	8
4	VIKING I Compact Burner	9
5	Combustion Chamber for Compact VIKING I Burner	10
6	Details of Injector Backplate for Compact Burner	11
7	Compact Burner Injector Assembly	12
8	Fuel Injector	13
9	Schematic of Injector Element Locations and Cooling Passages	15
10	Fuel Injector Flow Characteristics	16
11	Injector Spray Pattern	17
12	Schematic Block Diagram of the VIKING I Generator Test Facility	20
13	Test Facility Fuel and Oxidizer System Schematics	22
14	Test Facility Seed Feed System Schematic	24
15	Oscillograph Data for Run No. 12	28
16	Burner Heat Flux	29
17	Burner Heat Loss	30
18	Conductivity Channel	32

## SECTION I

### INTRODUCTION, SUMMARY AND CONCLUSIONS

This is the final report of Contract F33615-75-C-2047, "MHD Power Generation (VIKING Series) with Hydrocarbon Fuels", supported by the Defense Advanced Research Projects Agency and the United States Air Force Aero Propulsion Laboratory. The performance period for this contract was April 1975 to July 1975. The program was a continuation of a previous program aimed at advancing the state-of-the-art of high performance compact MHD generators. The earlier work is described completely in Ref. 1, and was performed in two parts:

- a) The VIKING I experimental program, using a two megawatt (nominal) high performance MHD generator.
- b) The VIKING II design program, to design a compact 10 MW MHD generator of about 2000 kg dry weight.

The current work had as its objectives the testing of a compact burner which was built as a model of a burner designed for the VIKING II 10 MW generator, and the subsequent operation of the VIKING I generator, using this burner. Only the first part of the program was completed, and this report is concerned primarily with the design, fabrication and testing of the burner.

The burner operating characteristics were governed by the requirements of the VIKING I generator, and are as follows:

Reactants:	Toluene ( $C_7H_8$ ) + Oxygen
Total Mass Flow:	2.7 kg/sec
Seed:	$Cs_2CO_3$ powder
Chamber Pressure:	15 atmosphere

The burner is started at full mass flow, and design pressure is reached in a few tenths of a second after the main fuel flow is started.

The burner was operated at mass flow rates and chamber pressures ranging from about 50% to 90% of design values. The mass flow rate was limited to 90% of design values by high pressure drops in the oxygen supply lines of the test facility. Heat losses at the highest mass flows were about 9% of the thermal input to the burner. The tests performed with the burner

provide useful information for the design of larger compact burners for lightweight MHD generators.

The burner design and fabrication are described in Section II of this report and the test program is described in Section III.



## SECTION II

### BURNER DESIGN, FABRICATION AND INSTALLATION

#### A. INTRODUCTION

The burner for the VIKING I facility was designed as a model of a burner for a prototype lightweight generator of 10 MW output. Although the VIKING I burner is not itself designed to be particularly light in weight, it was designed to achieve high performance in a compact size to allow the same design to be used in an enlarged version of lighter weight (per unit mass flow) for the 10 MW system.

The approximate operating conditions for the VIKING I burner are as follows:

Reactants:	$C_7H_8$ (Toluene) + gaseous $O_2$ + 1%-2% (mol) Cs
Combustion:	stoichiometric - 20% fuel rich
Mass Flow:	2.7 kg/sec (nominal) - 3.6 kg/sec (max.)
Stagnation Pressure:	15 atm (absolute)

#### B. OVERALL DESIGN CONSIDERATIONS

Requirements of an efficient compact MHD burner design are:

- 1) The attainment of rapid combustion rates in order to obtain complete combustion and hence, the greatest possible heat release rates in the smallest volume consistent with combustion stability and the structural integrity of the chamber;
- 2) The necessity of limiting heat transfer losses to the chamber walls;
- 3) A high degree of turbulent mixing to ensure uniformity of the distribution of seed at the channel entrance;
- 4) Uniform velocity and temperature profiles at the channel entrance to prevent degradation of MHD generator performance.

The importance of these requirements, which together determine the burner and seeding efficiency, may be seen from Figure 1, which shows measured variation of electrical conductivity of the combustion products with effective combustion chamber losses. The measurements were made in work reported in Ref. 1. It is seen that poor combustion chamber design can result in reduction of conductivity, and hence of generator power output, by a factor of two.

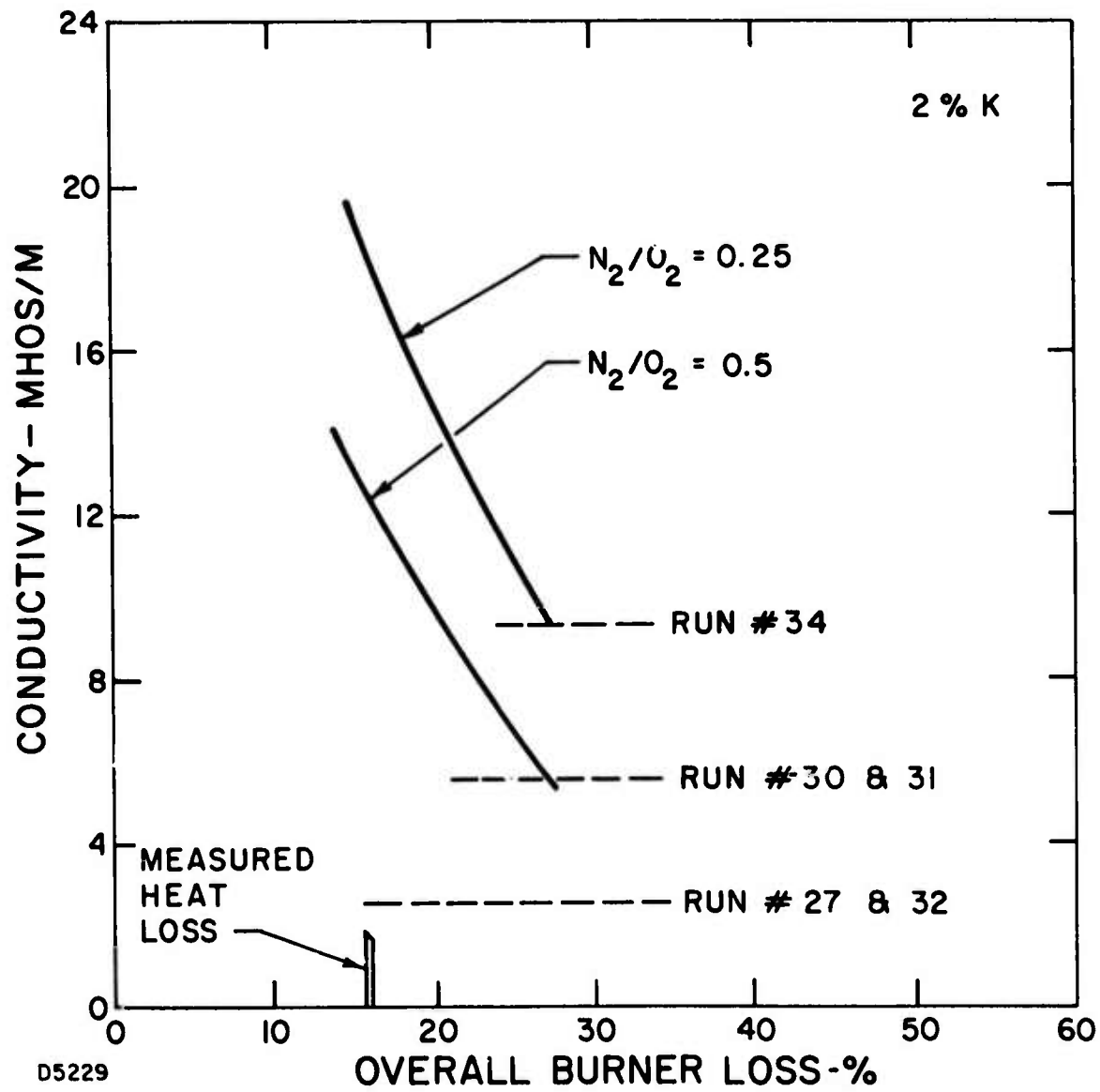


Figure 1 Conductivity as a Function of Overall Burner Loss

The third requirement, for a high degree of turbulent mixing, is important both for its effects on seed distribution and for its effects on combustion rates. For MHD burners, the importance of mixing rates lies primarily in their effects on seed distribution, since combustion rates are limited more by propellant vaporization rates than by mixing rates. It may be noted in passing that this requirement, together with the fourth marks a significant difference in design philosophy between MHD burners and rocket engines.

A relatively low risk approach was taken to the design of the compact VIKING I burner, without refinements which might later be necessary on a larger lightweight version. The basic design is a water cooled cylindrical can with the reactants injected axially at the upstream end. The inside diameter of the burner was designed to produce a mean bulk gas velocity corresponding to a Mach No. of about 0.1. The burner mates to the existing supersonic nozzle on the VIKING I generator. The contraction ratio is about 6. Emphasis was placed on the attainment of the maximum heat release rates in the smallest volume consistent with combustion stability and the structural integrity of the chamber. Because combustion rates are limited by propellant vaporization and gas-phase mixing rates, rather than by chemical reaction rates<sup>(2)</sup>, these rates can be used as a measure of combustion efficiency.<sup>(3,4)</sup> A high degree of mixing is less critical to combustor performance than is a high degree of vaporization, and can be more readily achieved in most designs. Hence, it was assumed that the performance of the burner is vaporization rate limited.

Vaporization rates for various combustion chamber design parameters can be calculated with a reasonable degree of confidence, assuming that reactant and combustion gas properties are known, and that the spray droplet size distribution at the injectors is also known. To a reasonable approximation, the effects of the nozzle are small, and since the contraction ratio and the chamber pressure have been previously fixed, the chamber length  $l_c$  necessary to obtain a given fraction of mass vaporization (combustion efficiency) is determined primarily by the mass mean drop radius  $r_m$  and the injection velocity  $v_o$ . Figure 2 shows the chamber length necessary to obtain given mass vaporization fractions, for a toluene spray, and for representative values of  $r_m$  and  $v_o$ . Since the burner is water cooled, the fuel injection temperature is approximately the same as the bulk water temperature, approximately (150°F).

The possibility of combustion instabilities was minimized by use of high velocity (momentum) ratios between the reactants, low injection densities, and the use of injectors with large reactant mass flow per element (i. e., few large elements rather than many small elements). The third requirement conflicts with the requirements of high combustion efficiency in short combustion chambers, since larger orifices tend to produce larger drops which take longer to vaporize.

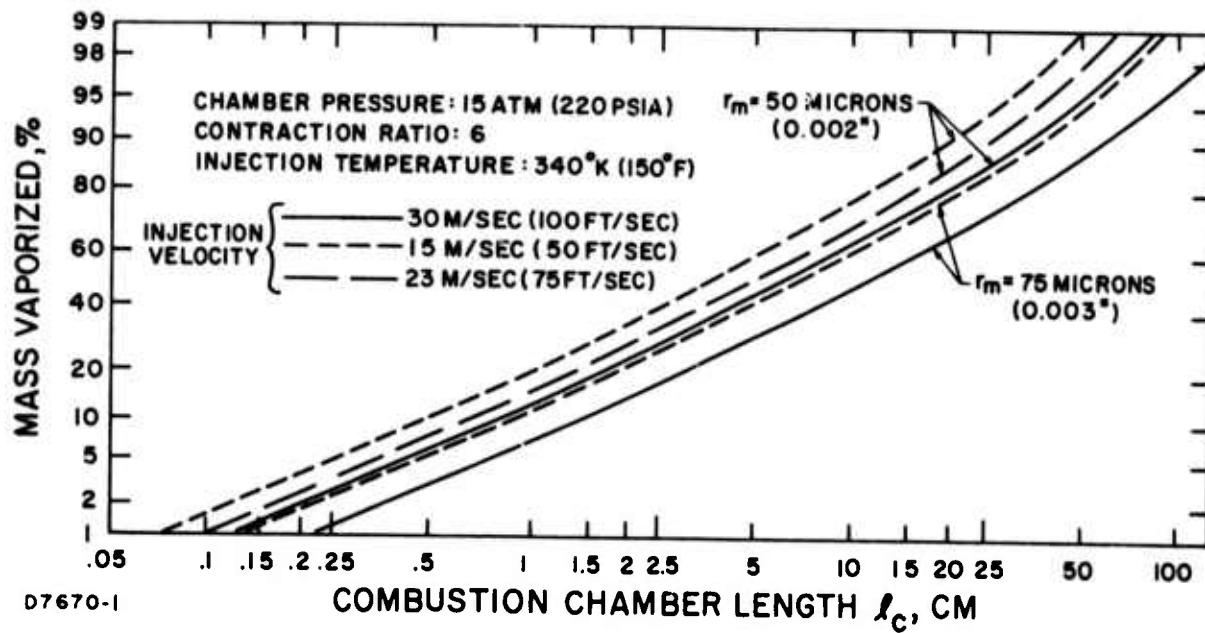


Figure 2 VIKING I Combustion Chamber Length

Low frequency (chugging) instability is prevented by high pressure drop across the fuel orifice and sonic gas injection velocity.

### C. DETAILED DESIGN

A diagram of the burner is shown in Figure 3, and a photograph in Figure 4. The main elements are the combustion chamber, the pilot burner and pilot ring, and the backplate, which is described in detail below. These members are flanged and bolted together for assembly. In lightweight versions, the flanges could be eliminated and the assembly could be welded.

The combustion chamber (Figure 5) is a water-cooled cylindrical tube wall design made of stainless steel, with an outer pressure vessel surrounding the tubes. Flanges on each end permit bolting to a supersonic nozzle (not shown) on the downstream end, and to the pilot ring and backplate on the upstream end. The combustion chamber was supplied by the Marquardt Company, Van Nuys, California. The inside diameter of the burner is 15.2 cm based on a desired mean gas velocity corresponding to a Mach No. of about 0.1. The burner mates to the existing supersonic nozzle on the VIKING I generator. The contraction ratio is about 6. The chamber length is 53 cm, based on design criteria discussed below in connection with the injector design.

The burner is ignited by means of a pilot burner, operating on  $\text{CH}_4 + \text{O}_2$  and fired by a spark plug. The pilot burner is water-cooled independently of the main burner, and is mounted in a water-cooled copper ring between the backplate and the combustion chamber. This location was chosen in preference to the backplate in order to avoid complicating the backplate design. The pilot ring serves also as a convenient location for burner instrumentation and possibly also for the introduction of powered seed.

The injector assembly is shown in Figures 6 and 7, and consists of the main housing, the faceplate and the fuel injection elements. The injector element configuration is coaxial, with the gas injected through the annulus and the liquid through the center tube. The main housing has machined into it an oxygen manifold, and originally contained also a fuel manifold. Use of the fuel manifold was abandoned in favor of a small external distributor, shown in Figure 8, feeding separately each fuel injector element, after cold flow tests showed that smooth starts and stops were difficult to achieve with the internal manifold.

The fuel nozzles (Figure 8a) are made of 304 series stainless steel, threaded into the main housing. Spacers near the tips serve to minimize vibration and to maintain alignment of the nozzles with the oxygen orifices. The fuel distributor is also shown in Figure 8. Connections from the distributor to the individual fuel elements are by means of flexible nylon tubing, clamped on to barbed fittings. The injector elements shown in Figure 8 were modified by the addition of extension tubes (Figure 8b) to accept the flexible hose.

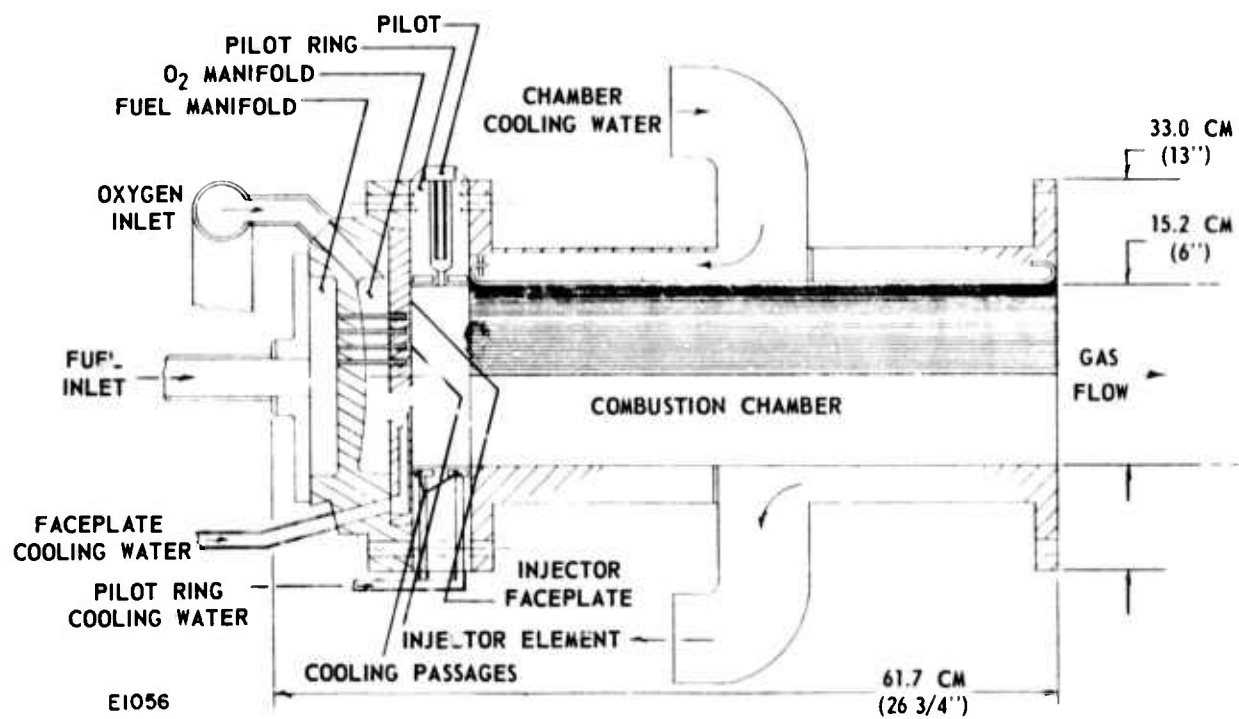


Figure 3 VIKING I Compact Burner

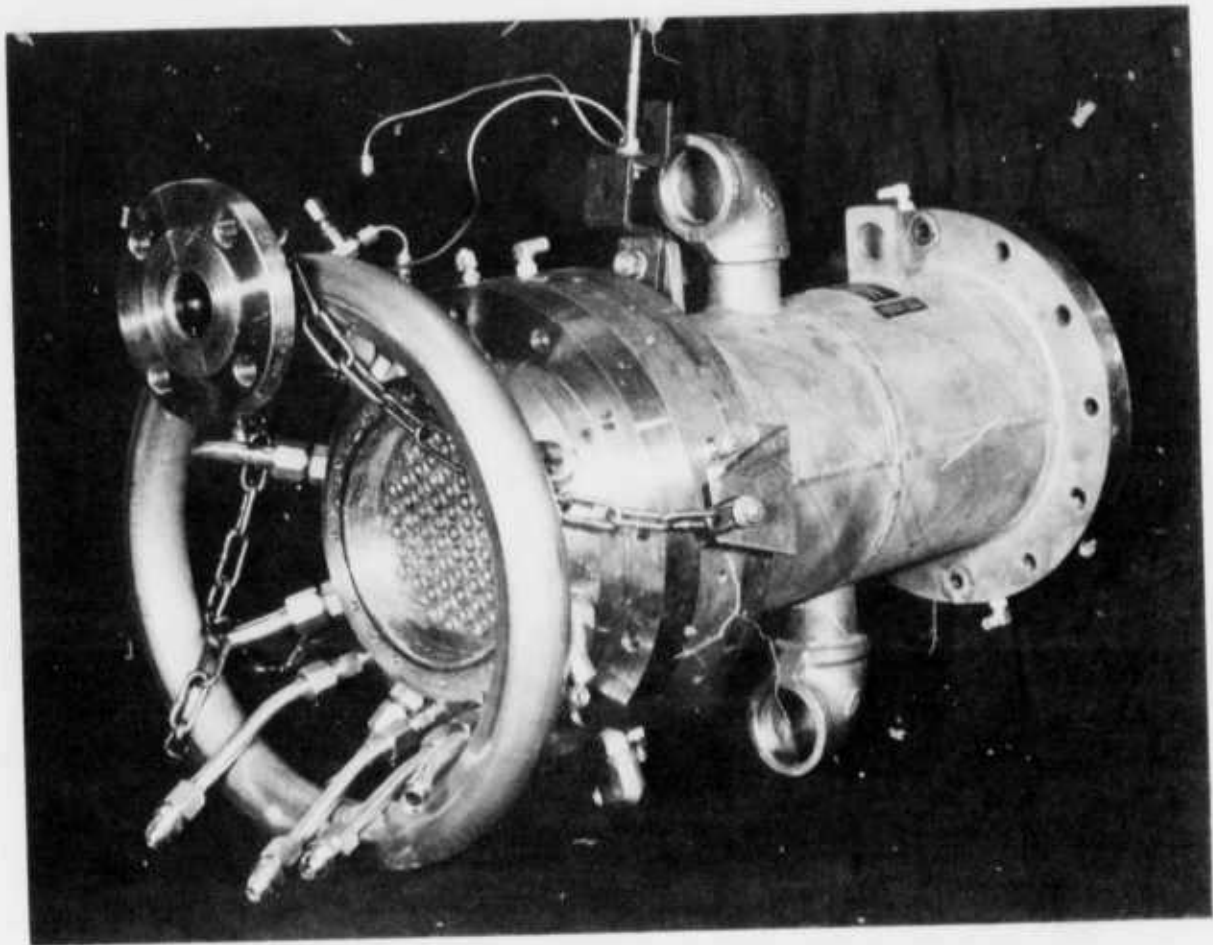


Figure 4 VIKING I Compact Burner

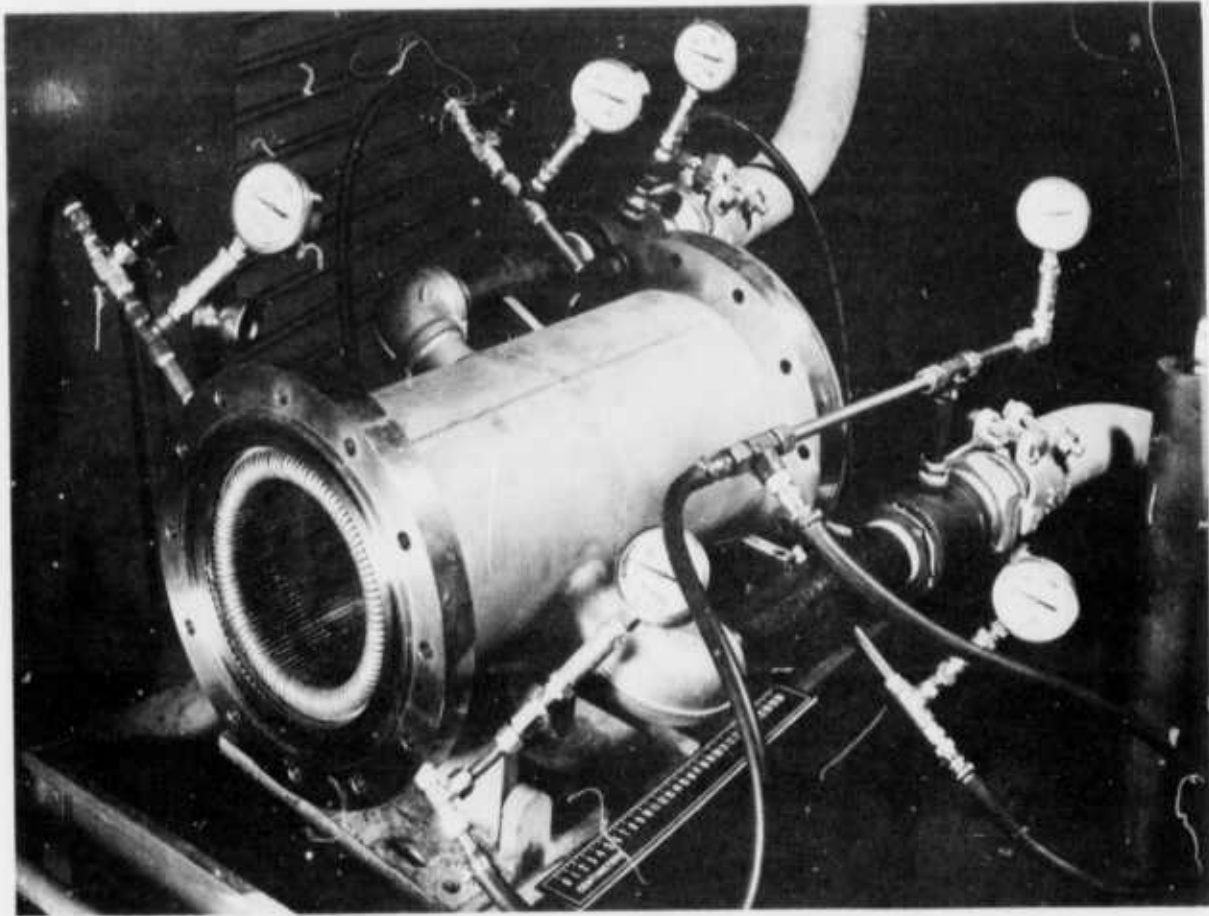
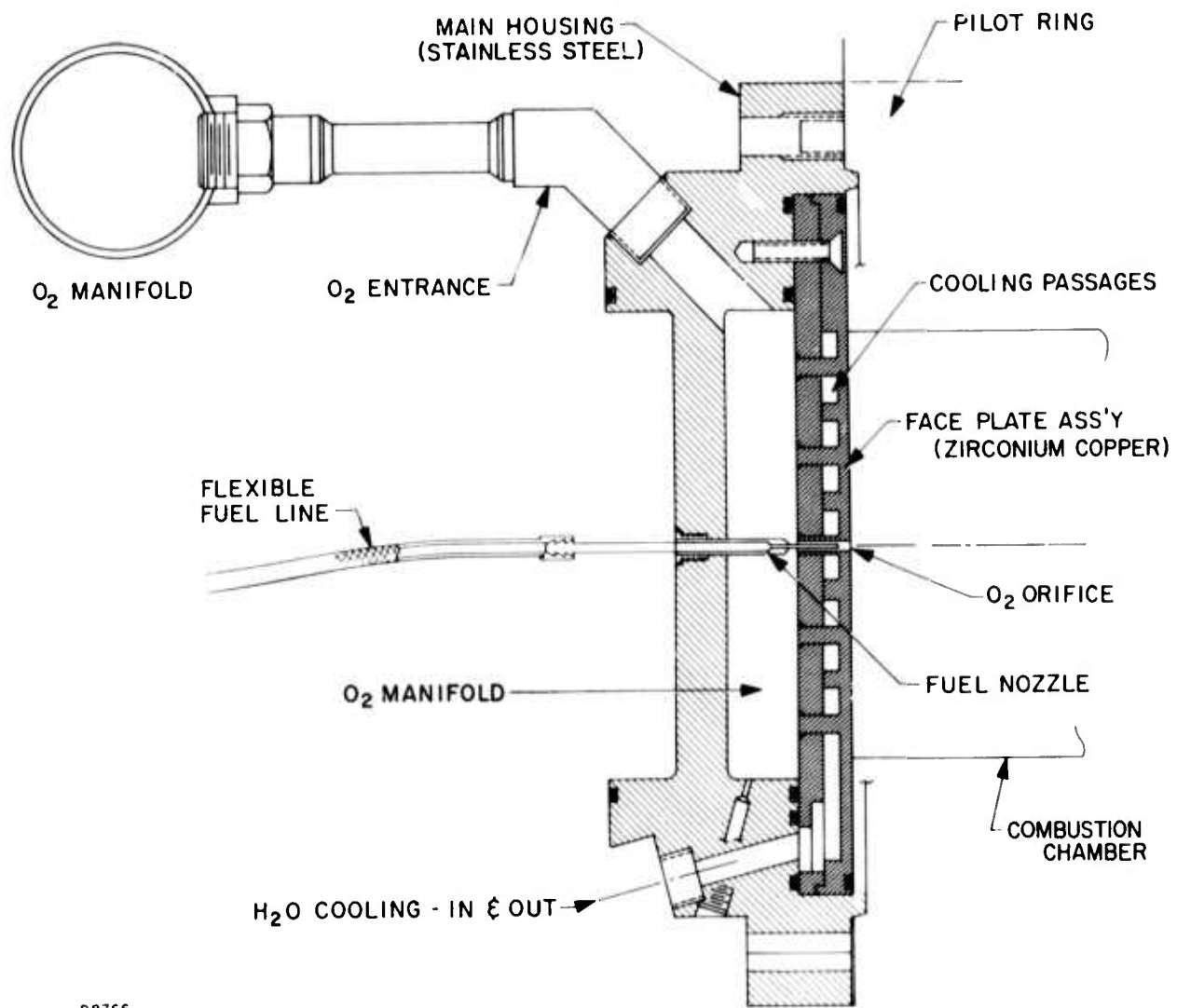


Figure 5 Combustion Chamber for Compact VIKING I Burner





08766

Figure 6 Details of Injector Backplate for Compact Burner

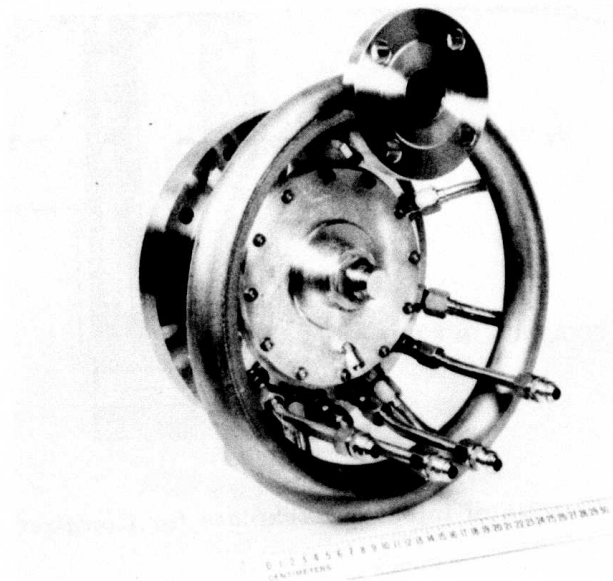
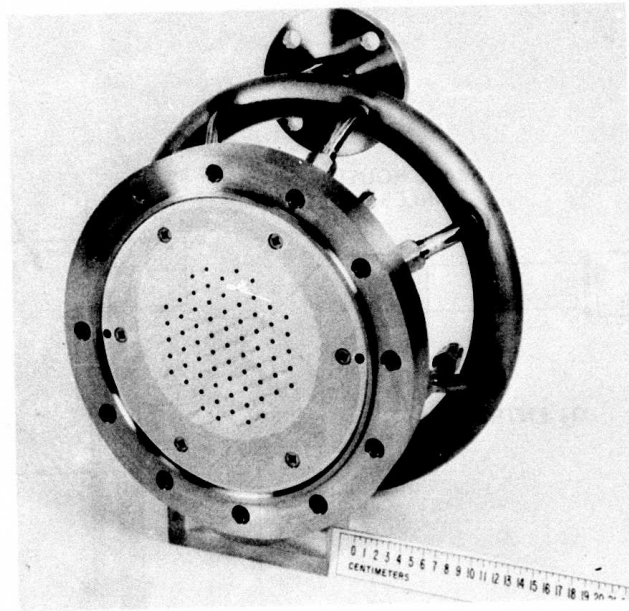
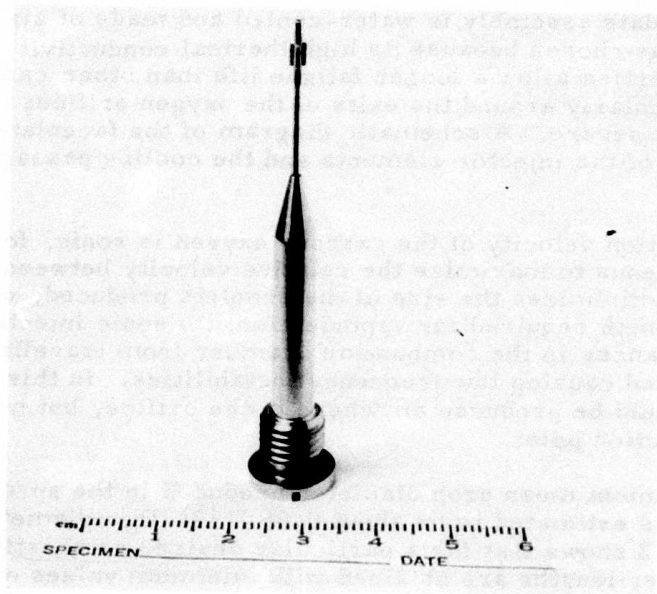
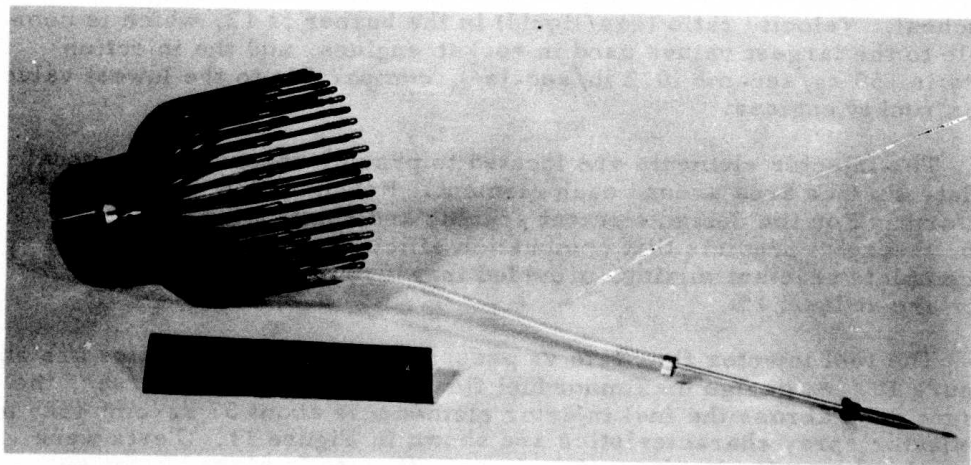


**Figure 7 Compact Burner Injector Assembly**  
**(a) Downstream View**  
**(b) Upstream View, Showing Cover and Inlet to Fuel**  
**Manifold which is no longer used**



(a) Fuel Injector Element



(b) Fuel Distributor

Figure 8 Fuel Injector

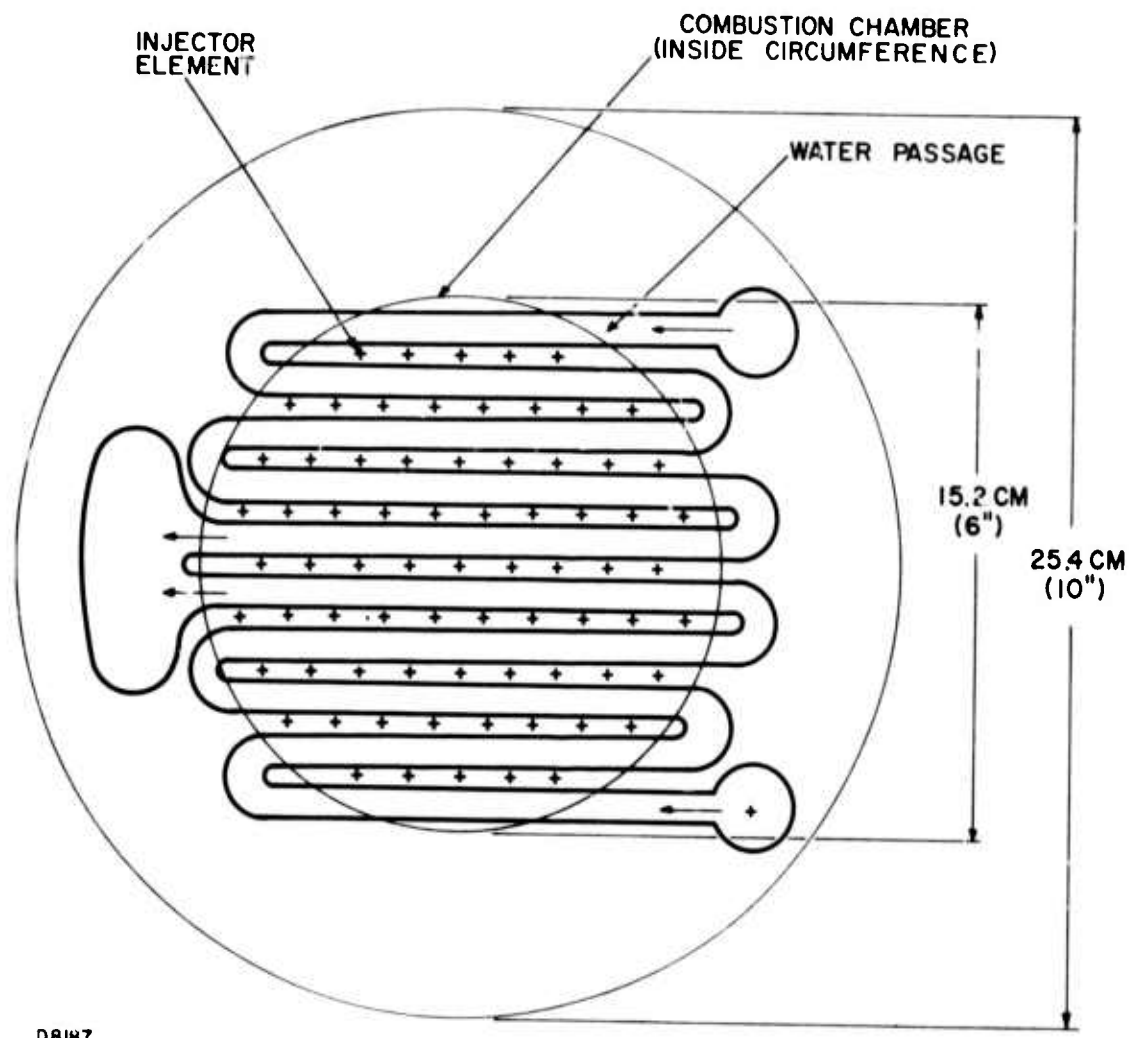
The faceplate assembly is water-cooled and made of zirconium copper, which was chosen because its high thermal conductivity and good mechanical properties allow a longer fatigue life than other candidate materials, particularly around the exits of the oxygen orifices where thermal stresses are severe. A schematic diagram of the faceplate, showing the arrangement of the injector elements and the cooling passages is shown in Figure 9.

The injection velocity of the gaseous oxygen is sonic, for two reasons: (a) it is advantageous to maximize the relative velocity between gas and liquid since this minimizes the size of the droplets produced, which in turn minimizes the length required for vaporization; (b) sonic injection prevents pressure disturbances in the combustion chamber from travelling upstream to the manifold and causing low frequency instabilities. In this case, the sonic velocity could be produced anywhere in the orifice, but most conveniently at the injection point.

The maximum mean drop diameter produced in the spray from this type of injector is estimated to be about  $0.06 D_o^{(5)}$  ( $D_o$  = diameter of the fuel orifice). Figure 2 shows that for a particular desired combustion efficiency, minimum chamber lengths are obtained with minimum values of mass median drop radius,  $r_m$ , and fuel injection velocity,  $v_o$ . The value of  $r_m$  was chosen to be 50 microns (0.002 inches), requiring a fuel orifice diameter  $D_o$  of 0.83 mm (0.032 inches). The fuel injection velocity was chosen as 23 m/sec, requiring 68 injection elements. For  $r_m = 50$  micron,  $v_o = 23$  m/sec and a desired efficiency of 98%, Figure 2 shows that the chamber length is 53 cm (21 inches). Velocity ratio (gas/liquid) in the burner is 13, which is comparable to the largest values used in rocket engines, and the injection density is  $150 \text{ kg/sec-m}^2$  ( $0.2 \text{ lb/sec-in}^2$ ), comparable to the lowest values used in rocket engines.

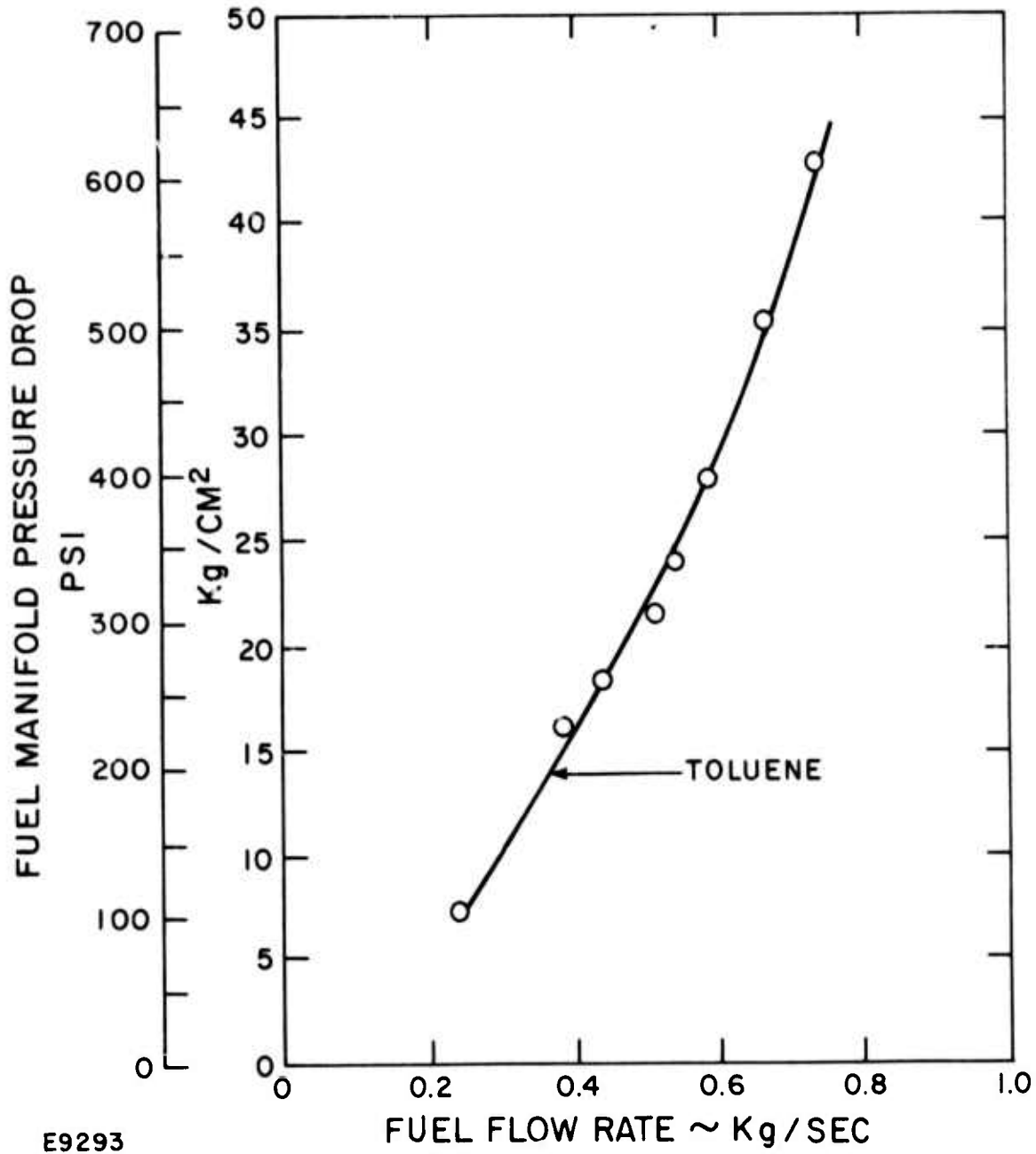
The injector elements are located to provide approximately equal faceplate surface area around each element. Reactant flow per element is uniform. For the design element spacing and combustion chamber length, theory<sup>(3)</sup> predicts that combustion efficiency will not be limited by incomplete reactant mixing, provided that turbulence levels in the burner are at least 1%.

The fuel injector flow rate vs pressure drop characteristics are shown in Figure 10. At design maximum fuel flow rate of about 0.7 kg/sec, the pressure drop across the fuel injector elements is about  $37 \text{ kg/cm}^2$  (525 psi). The injector spray characteristics are shown in Figure 11. Tests were conducted using water in place of fuel, and nitrogen in place of oxygen. The water mass flow rate was 0.7 kg/sec, and the gas manifold pressure was about 10 atmospheres, but the spray patterns and vaporization distances observed were qualitatively the same for all water flow rates and manifold pressures above 2 atmospheres. It can be seen from the photograph, that, with the gas flow, vaporization of the liquid jets occurred within 1-2 cm from the faceplate.



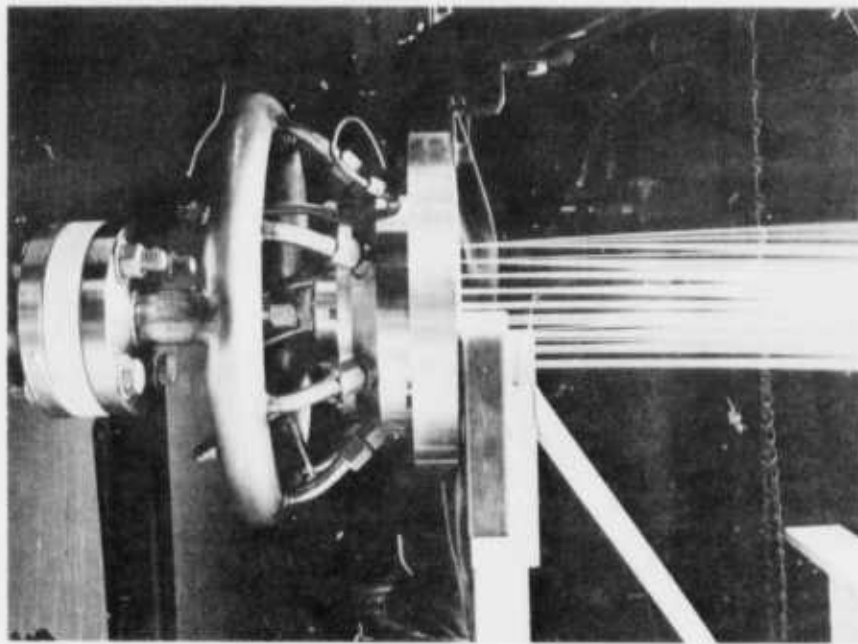
D8187

Figure 9 Schematic of Injector Element Locations and Cooling Passages

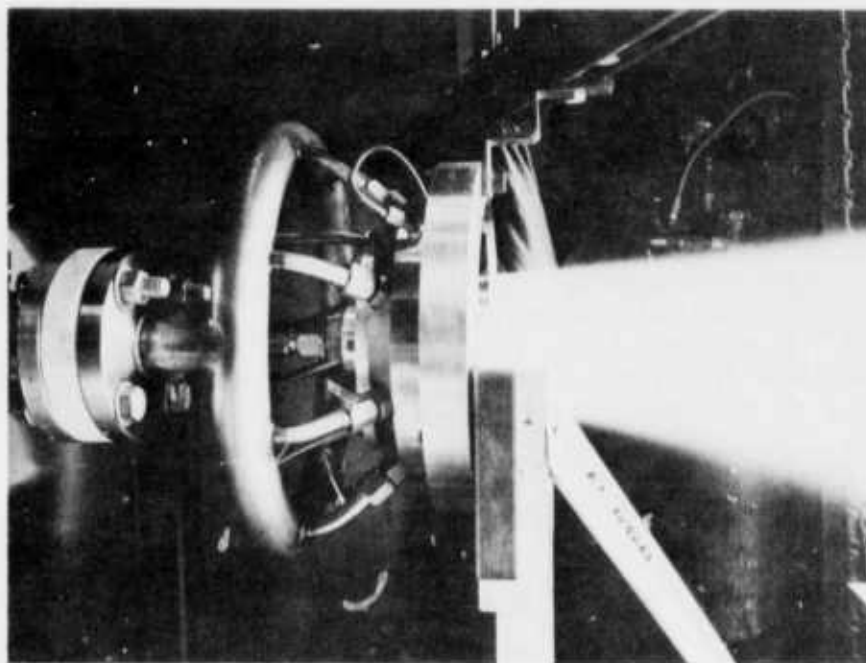


E9293

Figure 10 Fuel Injector Flow Characteristics



(a) Spray Pattern without Gas Flow



(b) Spray Pattern with Gas Flow

Figure 11 Injector Spray Pattern

The burner design is summarized in Table 1.

TABLE I  
BURNER OPERATING PARAMETERS

Design combustion efficiency	98%
Chamber diameter	15.2 cm (6")
Chamber length	53 cm (21")
Contraction ratio	6
Chamber pressure (nominal)	15 atm
No. of injector elements	68
Fuel orifice diameter	0.83 mm (0.032")
Oxygen orifice diameter	2.9 mm (0.115")
Fuel injection velocity	23 m/sec (75 ft/sec)
Mass median drop radius	50 micron (0.002")
Oxygen velocity	305 m/sec (1000 ft/sec)
Fuel/oxygen velocity ratio	13.3
Mass flow/injector element	0.04 kg/sec (0.088 lb/sec)

Seed injection to the burner can be either by means of a seed solution injected with the fuel, or by means of powdered seed injected through the faceplate using the oxygen as a carrier. The latter is the preferred method because higher conductivity is obtained. Tests of this method were conducted (using a small dummy faceplate) prior to fabrication of the faceplate, and results from the tests indicated that seed uniformity in the combustion chamber should be adequate and that blockage of oxidizer orifices by seed particles was not a problem. Also, the amount of seed settling in the gas manifold was small enough (<0.5% of the total throughput) so as not to affect measurably the seeding rate of the gas flow.

An alternate location for powder seed injection is the ring in which the pilot burner is mounted.



SECTION III  
TEST PROGRAM

A. TEST FACILITY

The test program was conducted in the existing VIKING I test facility, which is described below. Major operating parameters of the facility are as follows:

Total mass flow	2.0 - 3.6 kg/sec
Fuel	Hydrocarbons
Oxidizer	Oxygen or mixture of oxygen and nitrogen
Seed material	$\text{Cs}_2\text{CO}_3$ or $\text{K}_2\text{CO}_3$ (in powder form)
Burner pressure	$\leq 15$ atm
Cooling water flow	4000 to 8000 liters/min (1000 to 2000 gpm)
Run time	< 5 minutes

The run time of 5 minutes is governed by the storage capacities of fuel, oxidizer and seed.

The major subsystems of the test facility used in the current program are:

- Fuel System
- Oxidizer System
- Seed System
- Cooling Water System
- Exhaust System

Figure 12 is a block diagram of the test facility, showing the subsystems and their interconnections. The major subsystems are described briefly in the following.

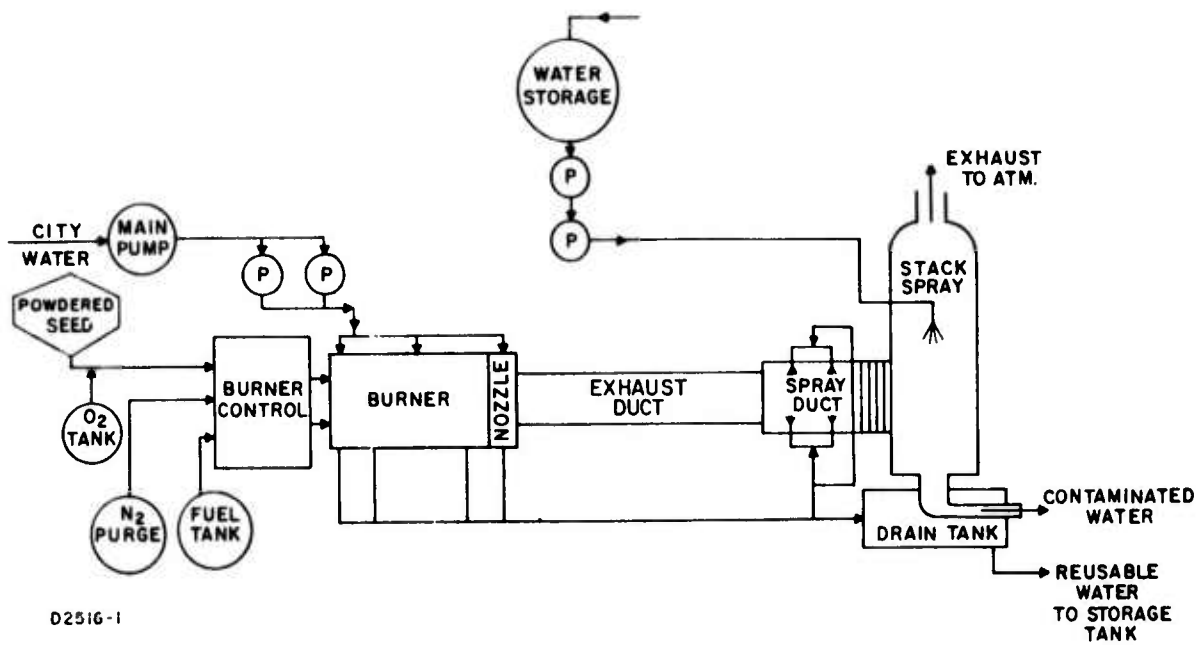


Figure 12 Schematic Block Diagram of the VIKING I Generator Test Facility

## 1. Fuel and Oxidizer Systems

A schematic of the fuel and oxidizer systems is shown in Figure 13.

The fuel system can use any hydrocarbon fuel such as #2 fuel oil or toluene. The fuel is stored in a 300 liter tank located outside the building. The tank is pressurized with nitrogen and the fuel flow rate, nominally 1 kg/sec, is controlled by varying the nitrogen pressure. The fuel flow is started when the oxidizer flow and pilot burner ignition have been established. To minimize startup time, the primary fuel control valve is located as close as possible to the fuel injection manifold of the burner. A second valve at the tank outlet closes automatically in event of an emergency shutdown. A relief valve is located on the fuel tank to prevent buildup of excessive pressure in the tank. A nitrogen purge is introduced to the fuel line at the control valve to blow excess fuel from the manifold after the control valve closes. Fuel flow rates are measured using a Daniel type turbine flow meter with an added preamplifier for accurate measurements at low flow rates.

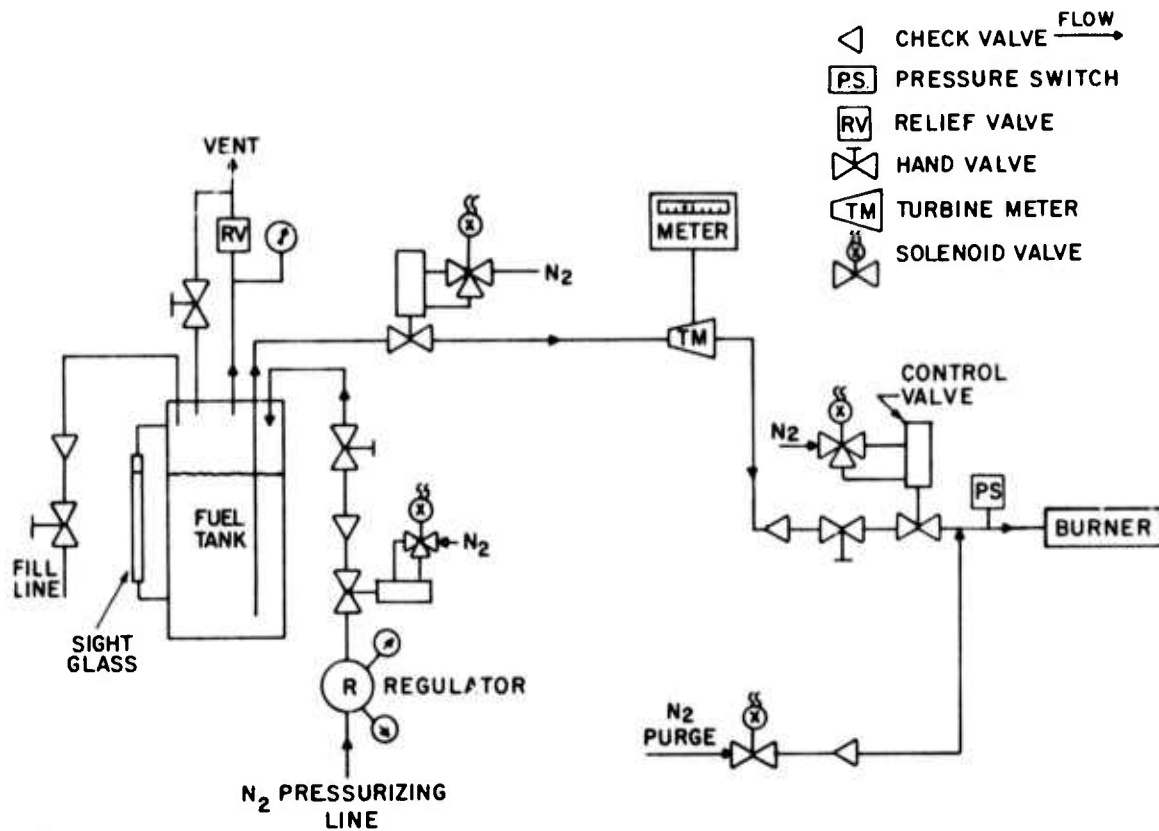
The oxidizer (pure oxygen) is stored in an 8.7 SCM tank rated at 160 atm, which feeds the test cell through a 10 cm drain pipe line. A hand-operated ball valve allows shutting off the oxygen to the test facility when oxygen is being used by other groups in the Laboratory. Oxygen flow rate is controlled by a throttling valve located on the roof and operated from the test facility control room. The throttling valve closes automatically in the event of an emergency shutdown. Final control of oxidizer flow is by a 5 cm remotely actuated ball valve located immediately upstream of the burner.

Burner ignition is by means of a pilot burner which operates on methane and oxygen, ignited by a spark plug.

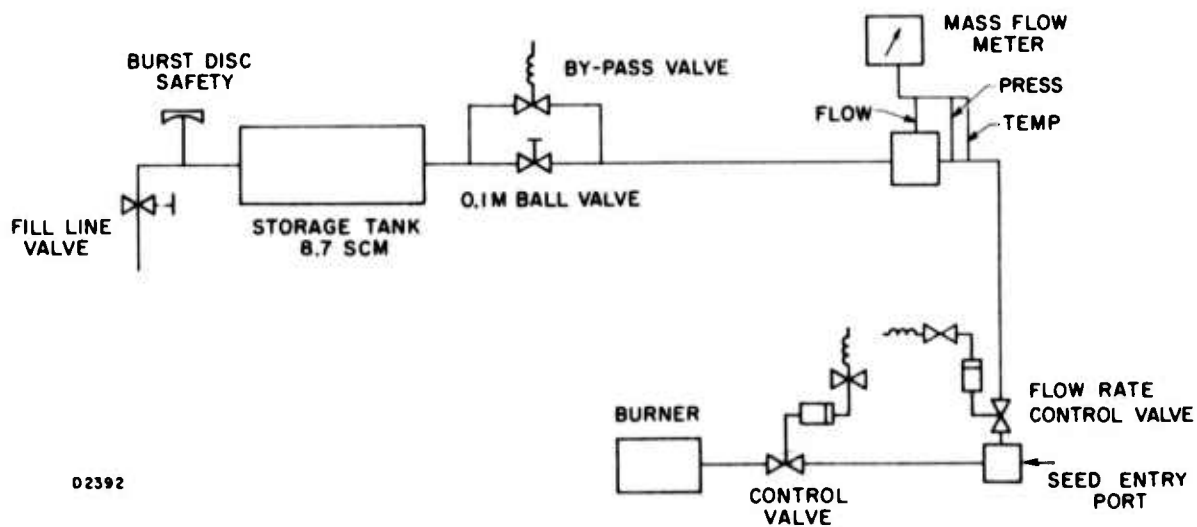
## 2. Cooling Water System

Cooling water to the test facility is supplied by a series and parallel water pump arrangement. Operation is either with city water alone or with a recirculating loop and a cooling tower. A schematic of the "city water" operational mode is shown in Figure 2. Cooling water for the burner and nozzle is supplied from the city water main at a nominal rate of 3200 liters per minute. The first stage pump is a 45 kW unit and the second stage consists of 37 kW units each supplying different system components at inlet pressures of about 20 atm.

Orifice plates and differential pressure gauges are located in the exit water lines to measure flow rates, and thermocouples are installed in the inlet and exit water lines to measure temperature rises. Thus, an energy balance of the system can be obtained. The burner is automatically shut down if the cooling water flow rate, pressure or exit temperature fall outside certain limits.



a) Schematic Diagram of Fuel System



b) Schematic Diagram of Oxidizer System

Figure 13 Test Facility Fuel and Oxidizer System Schematics

The spray duct is supplied with water at 4.1 atm via throttling valves located in the burner and nozzle outlet lines. Cooling water for the stack is supplied from a 7600 liter reservoir tank at a nominal rate of 3000 liters per minute. A 40-mesh strainer filters water from the tank prior to passage through a 2-stage pumping system. Replenishment of water for the reservoir tank is accomplished by an automatic makeup fill valve. "Clean" water can be cycled through the cooling tower and fed back into the reservoir tank. The "contaminated" water can be either put into the storm drain or it can be dumped into a settling bed.

### 3. Seed System

A schematic of the seed system is shown in Figure 14. The powder seed feed system consists of a seed hopper, 1 meter high and 0.33 meters in outside diameter, a rotor driven by a 0.746 kW DC motor with a 15-to-1 gear reduction box controlled by a speed controller through an electric clutch, and a remotely operated control valve. Either of two rotors can be used. Each is designed so that a range of seed flow from 0 to 6 weight percent of the total gas flow can be accommodated. The controller and motor are designed as a unit to make the seeder system compatible with a one-second startup of the MHD generator system. The powder seed is carried into the burner using nitrogen through the oxidizer line.

### 4. Exhaust Gas System

The exhaust gases from the burner flowed into an uncooled duct, leading to a 0.635 meter diameter steel spray duct (Figure 12) equipped with ten Spray Jet nozzles each with a capacity of 212 liters per minute at a pressure of 4.3 atm. Nozzles are staggered around the spray duct so that a fine mist of droplets penetrates as much of the exhaust gas as possible. The quenched gas enters a vertical exhaust stack tangentially and rises out of the facility. The exhaust stack is about 1.5 meters in diameter at its base and tapers down to 0.75 meter diameter at the roof. Additional quenching takes place in the stack some 3 meters above the gas entry point by means of a 758 lpm Spray Jet nozzle which points vertically downward.

## B. BURNER TESTS

Test instrumentation included pressure transducers in the main combustion chamber, the pilot burner chamber, and the main fuel and oxygen manifolds, thermocouples to measure cooling water temperature rise in the backplate assembly, the pilot ring, the combustion chamber and the nozzle, measurements of coolant flow in these components, and measurement of reactant flows to both the main burner and the pilot burner. Data were recorded on an eighteen channel oscillograph. A series of pilot burner tests were made prior to ignition of the main burner. Sample data are shown in Table II. Ignition of the main burner followed completion of

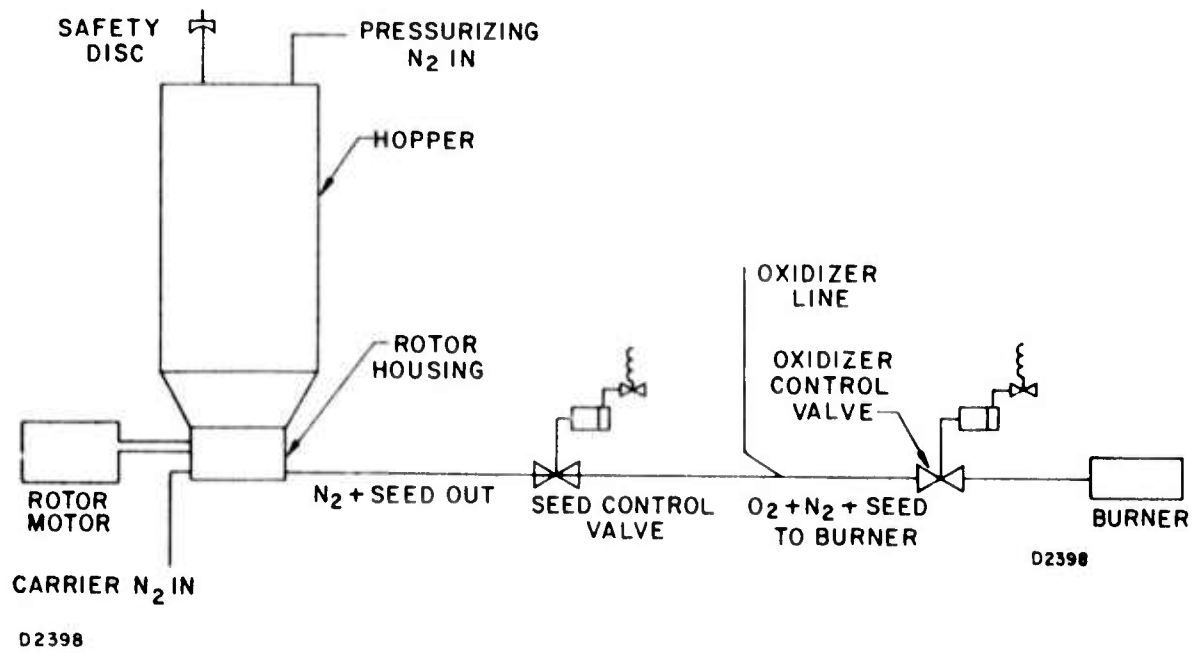


Figure 14 Test Facility Seed Feed System Schematic

TABLE II  
PILOT BURNER TEST PARAMETERS

O <sub>2</sub> Manifold Pressure (atm)	14.6	21.4	28.2	28.2	28.2	14.6	21.4	28.2	14.6	14.6	14.6
CH <sub>4</sub> Manifold Pressure (atm)	14.6	21.4	28.2	28.2	28.2	14.6	21.4	28.2	14.6	14.6	14.6
Chamber Pressure (atm)	7.8	11.5	16.0	16.0	16.0	7.8	11.6	14.6	7.8	7.8	7.8
Nominal Mass Flow Rate (gm/sec)	11.4	16.8	23.2	23.2	23.2	11.4	16.8	21.2	11.4	11.4	11.4
Run Duration (sec)	5.2	5.2	5.7	5.2	5.2	5.2	5.3	5.2	5.2	5.2	7.0
Cooling Water Flow (liter/min)	23.4	23.4	23.4	23.4	23.4	23.4	23.4	23.4	23.4	23.4	23.4
Cooling Water Temperature Rise (°C)	11.6	18.3	22.2	21.7	21.7	14.5	17.8	22.2	12.3	12.3	12.3

the pilot burner tests. Table III shows test conditions and results for the burner tests, and Figure 15 shows data for Run 12, which is typical of the other runs. Burner startup, operation and shut down were smooth in all cases, and the chamber pressure measurements show no traces of unsteadiness or oscillation. The rise time of the chamber pressure to full pressure is about 25 millisecc, to the first overshoot and about 0.25 sec to steady operation after the initial oscillations have damped.

The burner startup procedure is as follows. After coolant flows have been established, the main oxygen flow is started, followed by the pilot burner oxygen flow, pilot burner spark, and pilot fuel flow. At this point, the pilot burner is operating, and the main oxygen flow is established. The main fuel flow is then started, and main burner ignition occurs. Burner shutdown occurs in the reverse order. Figure 15 shows only the more important transducer traces, the less important traces having been omitted for the sake of clarity. The oxygen flow was fully established in the time interval shown in Figure 15, and so no deflection of the oxygen flow trace is seen.

Inspection of the burner after each test revealed no sign of structural damage or water leakage of the face plate or main chamber. Burner heat losses were measured by means of iron-constantan thermocouples in the exit water passages of the injector, pilot burner, pilot ring and combustion chamber, coupled with measurement of the cooling water flow rates in these components. Heat flux data for the injector plate and the combustion chamber are shown in Figure 16. Heat fluxes up to  $680 \text{ w/cm}^2$  were measured in the combustion chamber and up to  $880 \text{ w/cm}^2$  on the faceplate. The curves of heat flux vs mass flow rate vary approximately according to the 0.8 power of the mass flow density, as is to be expected. Heat flux data for the pilot ring are not shown because of the uncertainty in collecting area due to the exposure of part of both sides of the ring between the gas surface and the gas seal. Heat flux data for the nozzle are not shown because the nozzle operated in a semi-heat-sink mode, and the coolant temperature did not reach a steady-state value during a run.

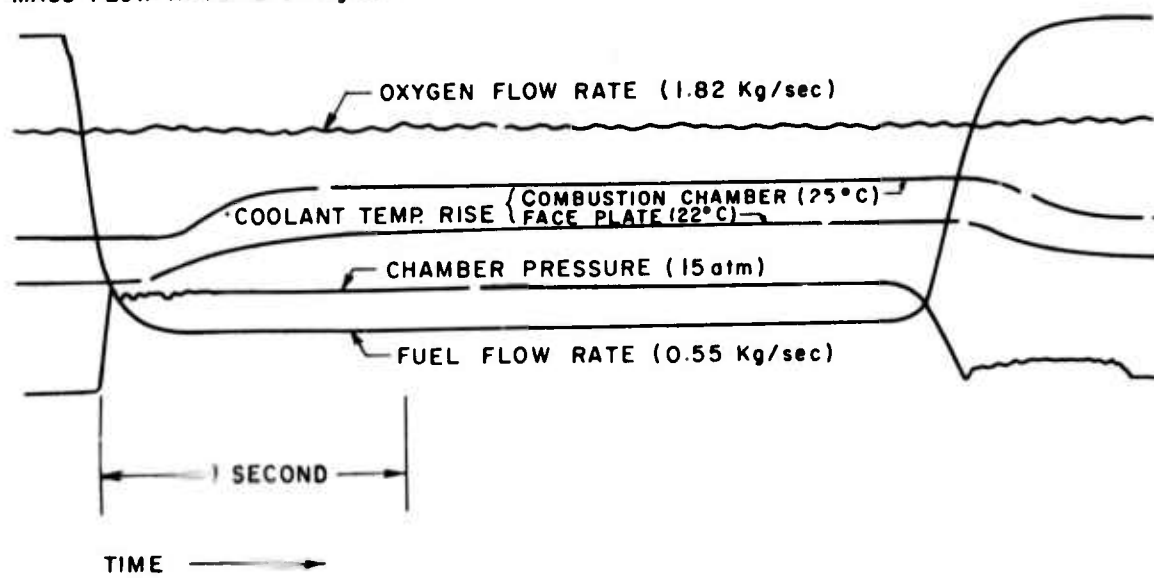
Heat loss data are shown in Figure 17, and at the high flow rates were about 9.3% of the burner enthalpy input. This is about half the value (of heat loss only) shown in Figure 1. The data of Figure 1 were obtained using a different burner, but at the same nominal Mach number and pressure as at the exit of the nozzle used in the current experiments. The reduced heat losses with the current burner result in an increase in conductivity, which can be estimated as follows. Other losses, resulting from incomplete combustion, non-uniform seeding, etc. are assumed the same as for the burner used to obtain the data in Figure 1. Using run 34 in Figure 1 as an example, it is seen that a conductivity of 9.3 mho/m was obtained with an overall burner loss of 27% and a measured heat loss of 17%. Under these conditions, an equivalent combustion/seeding efficiency of 88% can be calculated. Using this value, and a reduced heat loss of only 9.3%, as measured in the experiments reported herein, an overall efficiency of 80% is found, and an overall loss of 20%. Using this value, it is seen from Figure 1 that a conductivity of 14.3 mho/m can be expected, for a gain of 54% compared to the 9.3 mho/m obtained at the 17% heat loss. The



TABLE III  
COMPACT BURNER TESTS

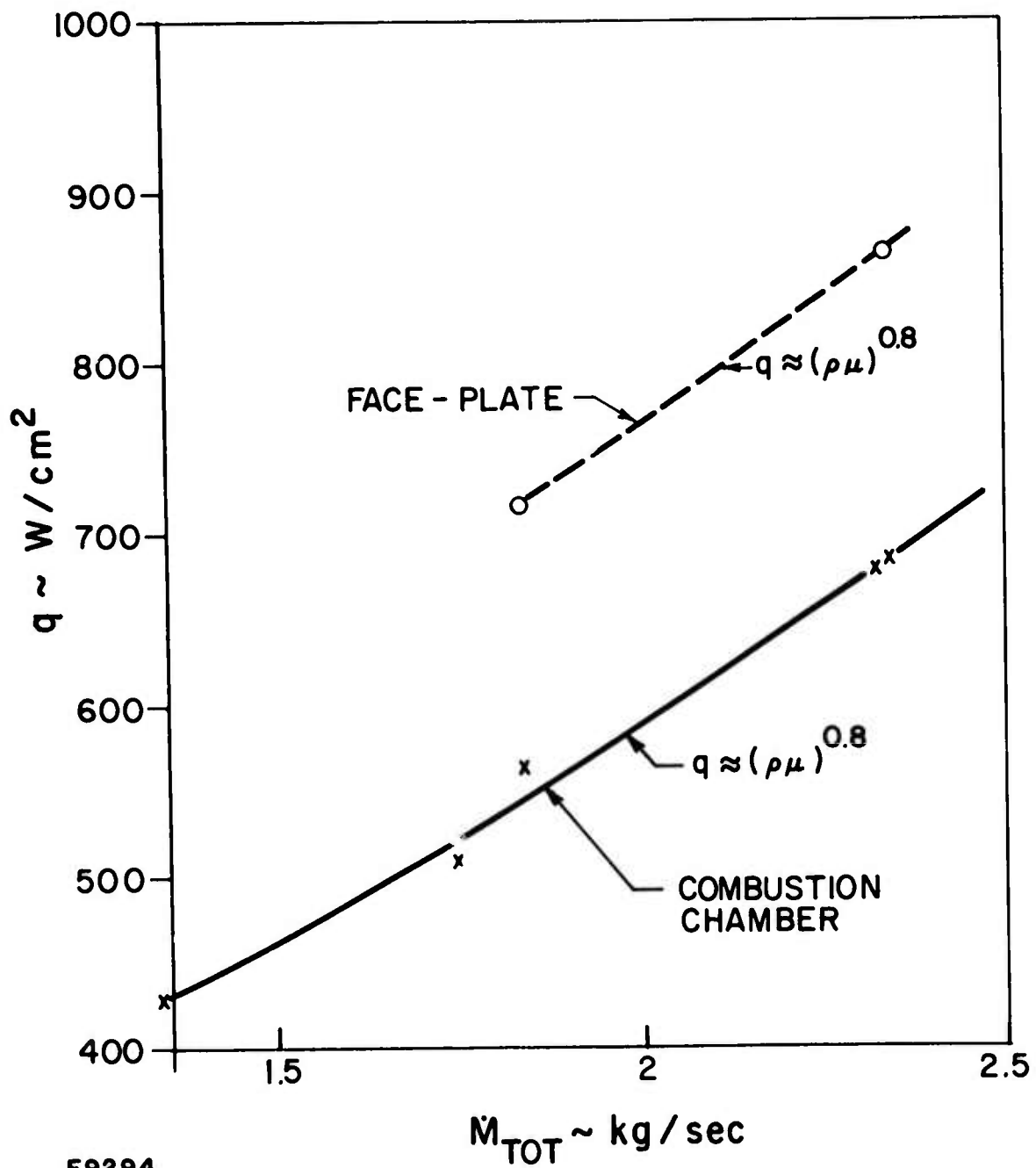
Test No.	Fuel	Oxidizer	Purpose of Test	Burner Mass Flow [kg/sec]	Chamber Pressure [Atm]	Run Duration [sec]	Comments
1	C <sub>7</sub> H <sub>8</sub>	O <sub>2</sub>	Checkout of burner at half design flow rate	1.28	8.0	1.2	Premature shutdown due to faulty interlock
2	C <sub>7</sub> H <sub>8</sub>	O <sub>2</sub>	Same as #1. Interlock fault corrected	1.28	8.0	3.1	Good run
3	C <sub>7</sub> H <sub>8</sub>	O <sub>2</sub>	Repeat of #2 to verify data	1.33	8.6	3.1	Good run
4	C <sub>7</sub> H <sub>8</sub>	O <sub>2</sub>	Increased mass flow rate to 2/3 design value	1.75	11.7	3.1	Burner ran smoothly. Faulty pressure transducer in fuel inlet line
5	C <sub>7</sub> H <sub>8</sub>	O <sub>2</sub>	Repeat of #4	1.82	--	1.2	Premature shutdown due to leak in chamber pressure line
6	C <sub>7</sub> H <sub>8</sub>	O <sub>2</sub>	Repeat of #5, leak repaired	1.83	11.4	3.1	Good run
7	C <sub>7</sub> H <sub>8</sub>	O <sub>2</sub>	Increase mass flow to maximum obtainable in facility	2.34	15.2	3.1	Burner ran smoothly. Malfunctions on some recorder channels
8	C <sub>7</sub> H <sub>8</sub>	O <sub>2</sub>	Same as #7. Corrected recorder malfunction	2.32	15.1	3.2	Burner ran smoothly. Some recorder channels still malfunctioning
9	C <sub>7</sub> H <sub>8</sub>	O <sub>2</sub>	Same as #8	2.28	14.9	3.0	Burner ran smoothly. Ringing on chamber pressure transducer trace
10	C <sub>7</sub> H <sub>8</sub>	O <sub>2</sub>	Same as #9. Replaced transducer	--	--	3.0	Ringing on all pressure transducer traces due to loose connections
11	C <sub>7</sub> H <sub>8</sub>	O <sub>2</sub>	Same as #10	2.4	15.1	3.1	Ringing reduced
12	C <sub>7</sub> H <sub>8</sub>	O <sub>2</sub>	Same as #11	2.37	16.1	3.0	Good run

REACTANTS:  $C_7H_8 + O_2$   
MASS FLOW RATE: 2.37 Kg/sec



E9296

Figure 15 Oscillograph Data for Run No. 12



E9294

Figure 16 Burner Heat Flux

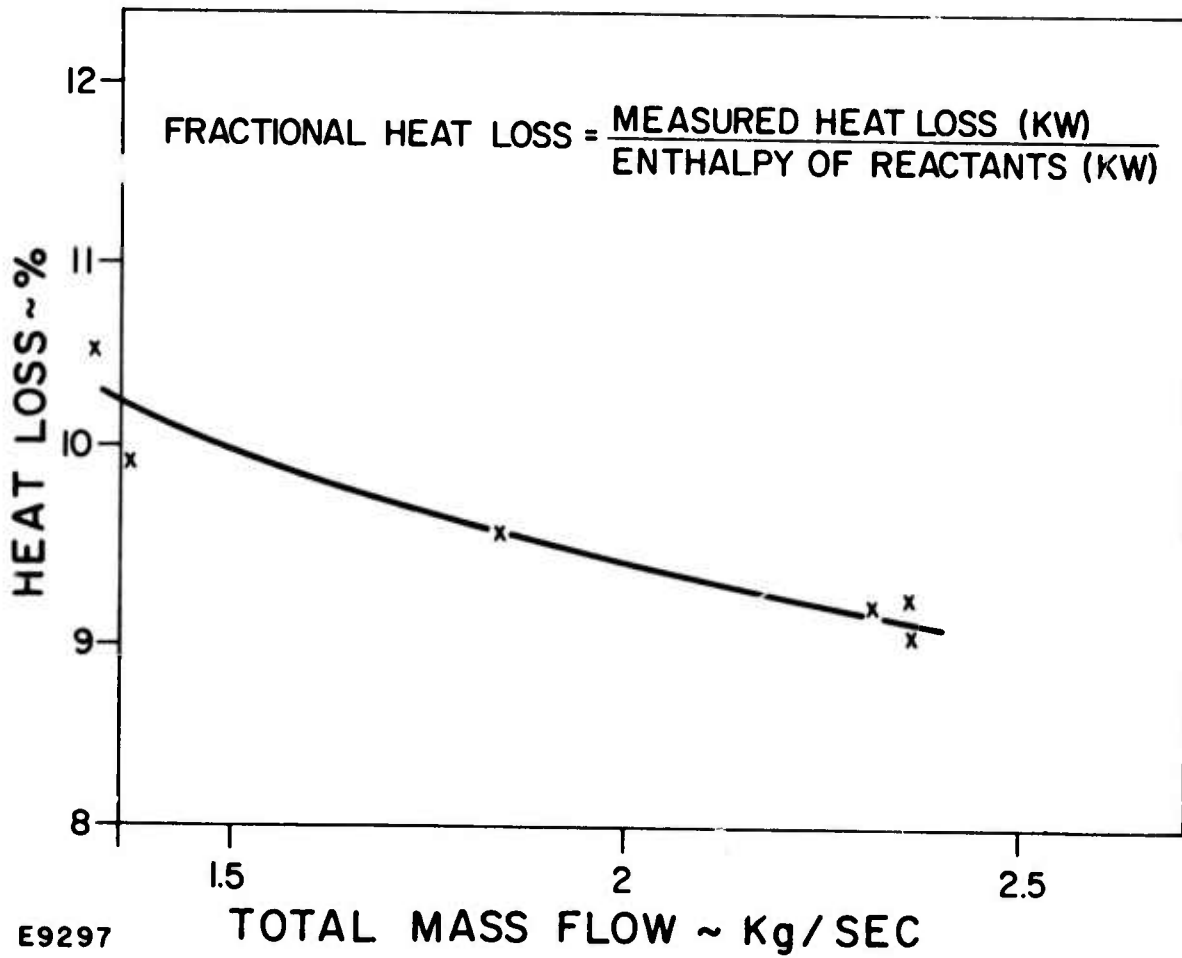


Figure 17 Burner Heat Loss

reference results in Figure 1 are with potassium seed and a  $N_2/O_2$  ratio of 0.25. With cesium seed, conductivities approximately double those with potassium seed can be obtained, or about 29 mho/m at the same N/O ratio as for run 34 in Figure 1. At lower N/O ratios the conductivity will be higher. Further, it is expected that combustion and seeding efficiencies are greater in the compact burner described in this report than the 88% estimated from Fig. 1, and it is estimated that a conductivity of about 35 mho/m can be obtained with cesium seed and pure oxygen.

### C. CONDUCTIVITY MEASUREMENTS

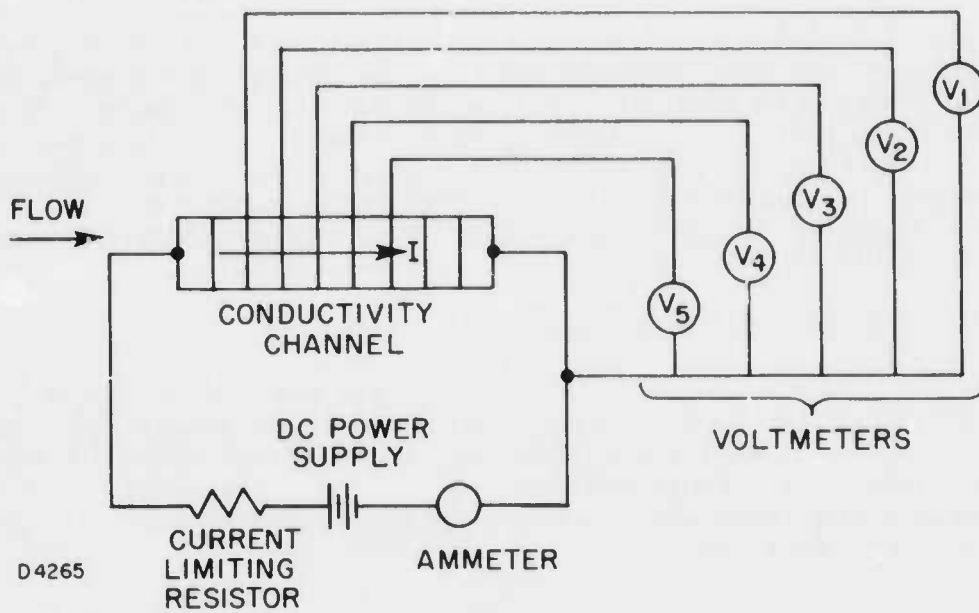
It had been planned as part of the current program to measure the electrical conductivity of the burner exhaust gas at the nozzle exit. The scheme to be used is shown in Figure 18a. An axial DC voltage is applied across a constant-area Hall-configuration channel. The current flow and axial voltage distribution are measured and the gas conductivity,  $\sigma$ , for a given channel length,  $\Delta X$ , is found from

$$\sigma = \frac{\Delta X}{A} \frac{I}{\Delta V}$$

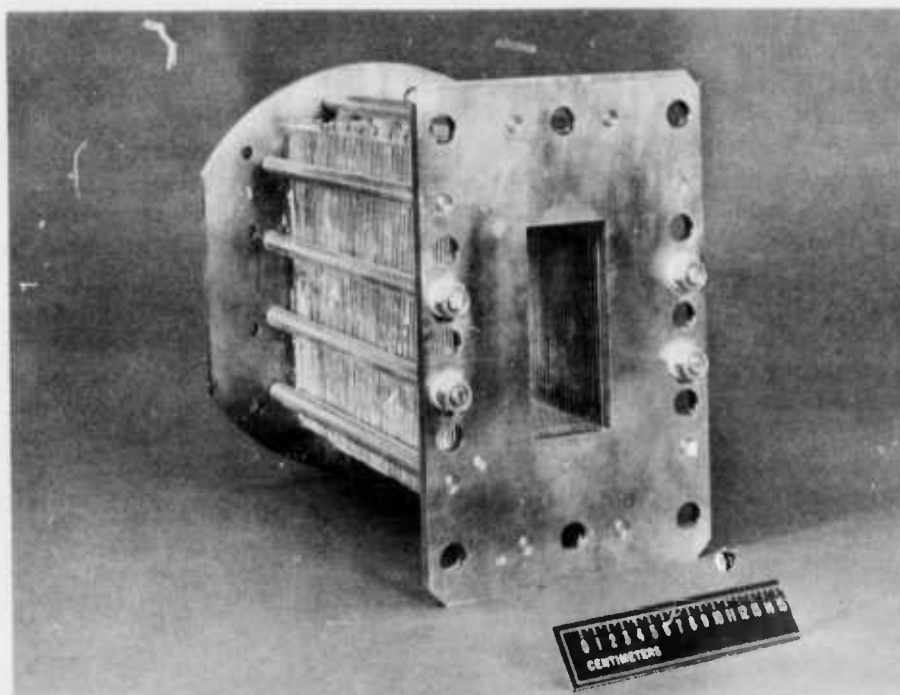
where  $I$  is the current in the circuit,  $A$  is the channel cross-section area, and  $\Delta V$  is the voltage across the length  $\Delta X$ .

A channel for this purpose was built (Figure 18b). The channel consists of alternating insulator and conductor modules held together by longitudinal tie bolts. The electrodes are made of copper, and the insulators of cast magnesia. The internal cross-section dimensions of the channel are 5 cm x 15 cm and the channel is 30 cm long. Each electrode module has an electrical terminal to enable its use for measuring the axial voltage distribution. In addition, a static pressure port is provided in the downstream flange of the channel to measure the operating static pressure.

Lack of time in the present program prevented performance of the conductivity measurements. Also, it was found that some components of the seed system were not suitable for operation at the high pressures required to feed the oxygen line, which operates at some 40 atmospheres pressure at high mass flow rates. This pressure is considerably greater than pressures operated previously in the facility, and the seed system will require some modification for use at such pressures.



a) Wiring and Instrumentation Diagram for Conductivity Tests



b) Assembled Conductivity Channel

Figure 18 Conductivity Channel

## REFERENCES

1. Kessler, R. , Sonju, O. K. , et al, "MHD Power Generation (VIKING Series) with Hydrocarbon Fuels", Final Technical Report AFAPL-TR-74-47, Part III, U. S. Air Force Aero Propulsion Laboratory, Wright-Patterson Air Force Base, Ohio, November 1974
2. Bittker, D. A. and Brokaw, R. S. , "Estimate of Chemical Space Heating Rates in Gas-Phase Combustion with Application to Rocket Propellants", ARS Journal, 30, 2 February 1960
3. Hersch, M. , "A Mixing Model for Rocket Engine Combustion", NASA TN D-2881 (1965)
4. Priem, R. J. and Heidmann, M. F. , "Propellant Vaporization as a Design Criterion for Rocket-Engine Combustion Chambers", NASA TR R-67 (1960)
5. Adelberg, M. , "Mean Drop Size Resulting from the Injection of a Liquid Jet into a High Speed Gas Stream", AIAA J. 6, 6 June 1968